Author(s): Jylhä, Liisi & Honkamo, Johanna & Jantunen, Heli & Sihvola, Ari

Title: Microstructure-based numerical modeling method for effective permittivity of ceramic/polymer composites

Year: 2005

Version: Final published version

Please cite the original version:

Jylhä, Liisi & Honkamo, Johanna & Jantunen, Heli & Sihvola, Ari. 2005. Microstructure-based numerical modeling method for effective permittivity of ceramic/polymer composites. Journal of Applied Physics. Volume 97, Issue 10. 104104/1-7. DOI: 10.1063/1.1897071.

Microstructure-based numerical modeling method for effective permittivity of ceramic/polymer composites

Liisi Jylhä, Johanna Honkamo, Heli Jantunen, and Ari Sihvola

Citation: Journal of Applied Physics **97**, 104104 (2005); doi: 10.1063/1.1897071
View online: http://dx.doi.org/10.1063/1.1897071
View Table of Contents: http://scitation.aip.org/content/aip/journal/jap/97/10?ver=pdfcov
Published by the AIP Publishing

Microstructure-based numerical modeling method for effective permittivity of ceramic/polymer composites

Liisi Jylhä[a)]
Electromagnetics Laboratory, Helsinki University of Technology, P.O. Box 3000, FI-02015 TKK, Finland

Johanna Honkamo[b)] and Heli Jantunen[c)]
Microelectronics and Materials Physics Laboratories and Electronics Materials, Packaging and Reliability Techniques Research Group of Infotech Oulu, P.O. Box 4500, FIN-90014 University of Oulu, Finland

Ari Sihvola[d)]
Electromagnetics Laboratory, Helsinki University of Technology, P.O. Box 3000, FI-02015 TKK, Finland

(Received 25 October 2004; accepted 1 March 2005; published online 29 April 2005)

Effective permittivity was modeled and measured for composites that consist of up to 35 vol % of titanium dioxide powder dispersed in a continuous epoxy matrix. The study demonstrates a method that enables fast and accurate numerical modeling of the effective permittivity values of ceramic/polymer composites. The model requires electrostatic Monte Carlo simulations, where randomly oriented homogeneous prism-shaped inclusions occupy random positions in the background phase. The computation cost of solving the electrostatic problem by a finite-element code is decreased by the use of an averaging method where the same simulated sample is solved three times with orthogonal field directions. This helps to minimize the artificial anisotropy that results from the pseudorandomness inherent in the limited computational domains. All the required parameters for numerical simulations are calculated from the lattice structure of titanium dioxide. The results show a very good agreement between the measured and numerically calculated effective permittivities. When the prisms are approximated by oblate spheroids with the corresponding axial ratio, a fairly good prediction for the effective permittivity of the mixture can be achieved with the use of an advanced analytical mixing formula. © *2005 American Institute of Physics*.
[DOI: 10.1063/1.1897071]

I. INTRODUCTION

Ceramic-polymer composites consisting of ceramic crystal particles in an amorphous background material have several interesting properties. Their electrical properties, including effective permittivity, can be adjusted by changing the fractions of the constituents. Furthermore, these materials have a plasticlike nonfragile structure and are suitable for multilayer structures even in curved shapes. Recently, ceramic-polymer composite materials have been studied in various applications, such as integrated decoupling capacitors,[1] angular acceleration accelerometers, and acoustic emission sensors.[2]

An obvious method to estimate the effective dielectric properties of a composite with a given composition is to apply classical mixing formulas and effective-medium theories, such as the Maxwell Garnett or Bruggeman models.[3,4] These, at least in their basic forms, have limitations and are certainly not universal for mixtures and composite materials of all types, and they sometimes fail, especially when the composite has marked permittivity contrasts between its components.[5] More advanced effective-medium theories require parametric fitting. However, these parameters are not known *a priori*. It quite often happens that, in experimental and fabrication works, one needs to resort to a trial-and-error procedure in the search for correct mixing ratios. This can be very laborious. There is clearly a need for more detailed mixing models that take into account the microstructure of the composites better than the classical mixing rules do. This would provide a reliable method and an effective modeling tool for designing materials.

With constantly increasing computational capacity, one is able to solve numerically larger electromagnetic problems involving inhomogeneous dielectrics. The recent literature contains several reports of efforts to develop different numerical approaches to predict the effective permittivity of disordered mixtures. In Refs. 6 and 7, much attention has been focused on the avoiding of the effect of periodicity. The mixture analyzed consists of a three-dimensional chessboard-type structure, where elementary cubes are filled with inclusion or background material. The computation domain contains a large number of inclusions, and this leads to the limitation that the fine structure cannot be modeled realistically.

Another possibility is to give more attention to the inclusions themselves in the numerical model. Calculations have been made in two and three dimensions using spherical[8–10] or cubical[11] inclusions. Effective permittivity as a function of the volume fraction of inclusions appears to be highly depen-

[a)]Electronic mail: liisi.jylha@tkk.fi
[b)]Electronic mail: jhonkamo@ee.oulu.fi
[c)]Electronic mail: heja@ee.oulu.fi
[d)]Electronic mail: ari.sihvola@tkk.fi

dent on the shape of inclusions. Thus, these simulations predict different dependencies on the volume fraction of inclusions.

Most of the reported numerical studies lack any comparison of the results with measured values. Furthermore, those that include such comparisons[7,8] do not report a very good agreement with the measured data in all volume fractions of inclusions. This is often because they do not take into account the fine structure of the material. It is not sufficient to model the mixture as a type 0-3 composite as such. Rather, the shape of the elementary inclusions needs to be modeled as well. The label "0-3 composite" refers to a structure in which the ceramic component is not continuous in any direction, whereas the polymer is continuous in all of the three directions. The simplest model for type 0-3 composites, from a numerical point of view, is a chessboardlike structure.[12] The fine structure of ceramic powder in epoxy is, however, different because ceramic inclusions in the epoxy resin have a geometry very different from the assumption of aligned and randomly distributed cubics.

In Ref. 13, the mixture was modeled with a cubic lattice of aligned cylinders. This model involves several parameters fitted to achieve a match with the measurements. The method is in good agreement with the measured data, but has the shortcoming that the parameters are material sensitive. If the ingredients and the microstructure of the mixture are changed, there is no guarantee that the model will apply accurately any longer.

In this study, we concentrated on the measurement and modeling of the effective permittivity of 0-3 ceramic/polymer composites. The prepared samples consisted of randomly dispersed TiO_2 inclusions up to 35 vol % in an epoxy matrix. The model to determine the dielectric properties is based on Monte Carlo simulations using a reasonably small calculation domain compared to the size of the ceramic particles. The parameters that are required in the numerical implementation are solved from the lattice structure of TiO_2. These same parameters are also used in advanced effective-medium models, which approximate the shape of inclusions with ellipsoids. Measured and modeled permittivity values are compared.

II. EXPERIMENTAL PROCEDURE

A. Equipment

Titanium dioxide, with a composition of a minimum 97% rutile phase (Merck), was used with a solution of epoxy (bisphenol-A) and curing agent (triethyleneamine) (Struers) as starting materials to form the slurry for bulk composite samples. Composites with ceramic loadings of 10, 15, 20, 25, 30, and 35 vol % were prepared. After mixing and vacuum treatment, the slurry was poured into cylindrical molds. The composite samples were cured in air for 24 h. Sample densities were estimated from the physical dimensions and weights of polished samples. Electrodes were painted on both sides of the cylinders by using conductive silver paint (Electrolube). Capacitances were measured with a HP4284A precision *LCR* meter (Hewlett-Packard, USA) in the frequency range of 10 kHz–1 MHz. The height of the cylinder h compared to the surface area A was approximately $h/A \approx 0.01$. The stray fields outside the sample were assumed to be negligible, leading to the following estimate of the effective permittivity of a sample:

$$\epsilon = \frac{Ch}{\epsilon_0 A}, \tag{1}$$

where C is the measured capacitance and ϵ_0 is the permittivity of vacuum.

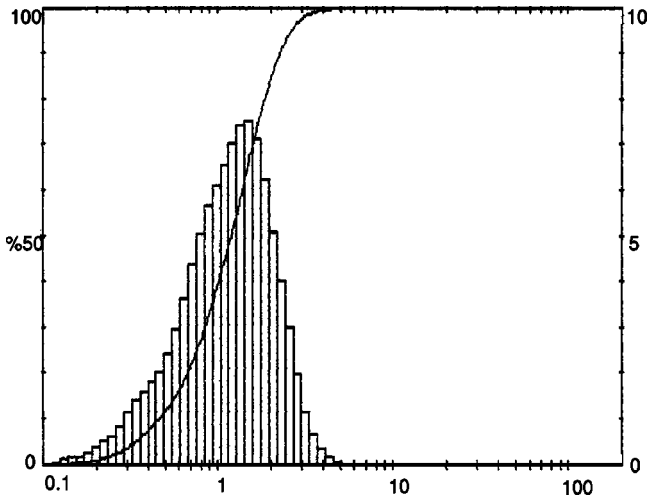

FIG. 1. Particle size distribution of TiO_2 powder in micrometers.

The particle size distribution of the titanium dioxide powder was measured with Malvern Mastersizer (MS1002, Malvern Instruments Ltd., Malvern, UK). The particle morphology and microstructure of the composites were studied with a scanning electron microscope (SEM) (Jeol JEM-6400, Tokyo, Japan).

B. Material parameters for modeling

The analysis of the sample structure yielded essential input data to enable accurate modeling of permittivity. Several experimental parameters were determined. The particle size distribution (Fig. 1) of TiO_2 powder showed marked deviation with a D_{50} value of 1.18 μm. Similarly to size, the shapes of individual particles were also diverse (Fig. 2). The microstructures of the composite samples with ceramic loadings of 10 and 25 vol % are shown in Figs. 3 and 4, respectively. The white area represents the titanium dioxide phase,

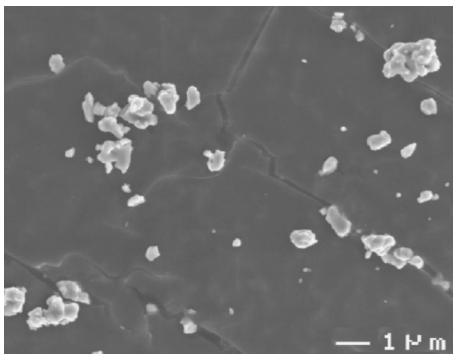

FIG. 2. Scanning electron microscope image of TiO_2 powder.

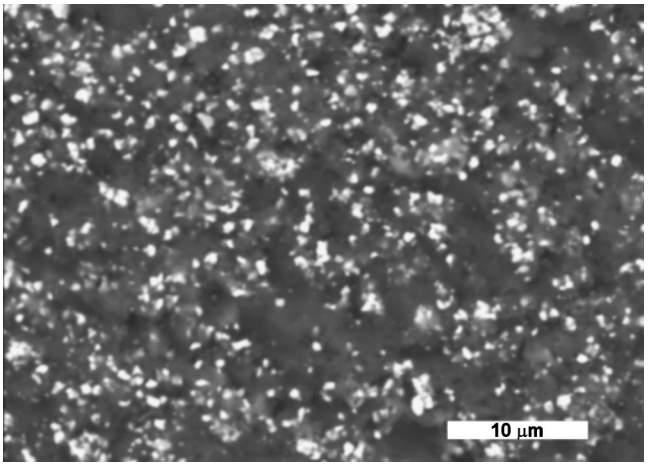

FIG. 3. Microstructural image of ceramic/epoxy composites with a ceramic loading of 10 vol %.

while the dark areas correspond to epoxy resin. The figures show that TiO_2 particles are well dispersed, although some overlap also exists, especially with large mixing ratios. In order to avoid the formation of air bubbles, special attention was paid to sample preparation by keeping the samples in a vacuum chamber. Despite these precautions, it was noticed at the stage of polishing the samples that some air bubbles were present. This was especially obvious at large mixing ratios.

The measured permittivities of pure epoxy and composites with ceramic loading of 10–35 vol % are shown in Fig. 5. The results show that the addition of TiO_2 modifies considerably the permittivity of pure epoxy. At 1 MHz, the permittivity of pure epoxy is 3.7, while a ceramic loading of 30 vol % increases the value of permittivity to 11.0. The same trend can be seen at all frequencies.

Permittivity was measured for $4\cdots6$ parallel samples at room temperature. The standard deviation in the permittivities for each volume fraction of TiO_2 powder is

$$s = \sqrt{\frac{\Sigma_{n=1}^{N}(\epsilon_n - \hat{\epsilon})^2}{N-1}}, \tag{2}$$

where N is the number of parallel samples, $\hat{\epsilon}$ average permittivity, and ϵ_n the permittivity of each sample. The main error

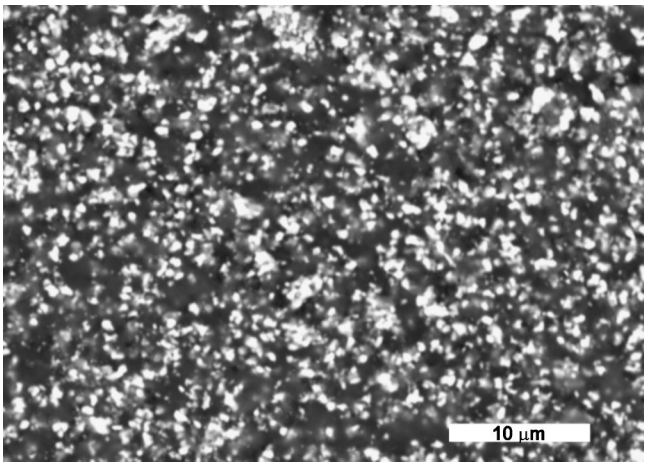

FIG. 4. Microstructural image of ceramic/epoxy composites with a ceramic loading of 25 vol %.

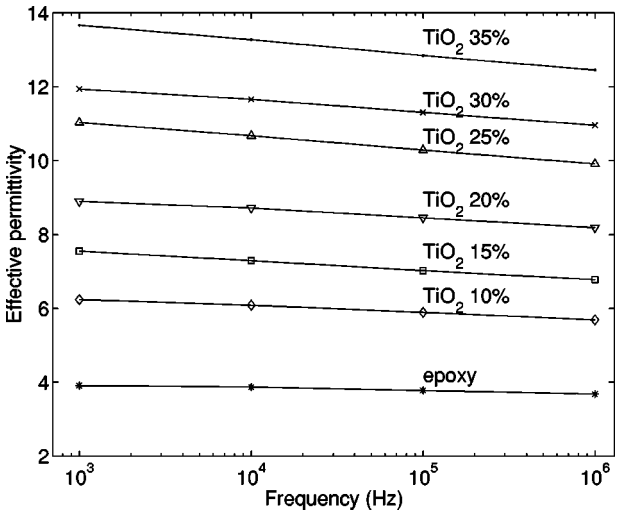

FIG. 5. Relative permittivity of epoxy and composites with ceramic loadings of 10, 15, 20, 25, 30, and 35 vol % as a function of frequency.

source is the uncertainty of the volume fraction of TiO_2 in epoxy. [Deviation according to (2) of the measured permittivities is shown later in Figs. 9 and 10.]

III. MODELING PROCEDURE

The permittivities of all the present phases are needed for modeling. For the inclusion phase, the average value for the relative permittivity of anisotropic TiO_2 inclusions was used: $\epsilon_i = (\epsilon_{xx} + \epsilon_{yy} + \epsilon_{zz})/3 = 114$.[14,15] The permittivity of epoxy depends on the frequency, but that of rutile remains practically the same in the frequency range of 100 kHz–1 MHz used here. For numerical simulations, the frequency was chosen to be 1 MHz. At this frequency, the relative permittivity of epoxy is $\epsilon_e = 3.7$. The size of inclusions was determined to be much smaller than the wavelength and the measured loss tangent of TiO_2/epoxy was moderately small (0.02). Accordingly, static simulations were used, and only the real part of the effective permittivity of the TiO_2/epoxy composite was solved.

A. Modeling principle

The composite was modeled using three-dimensional Monte Carlo simulations. A schematic layout of the computation domain is presented in Fig. 6. Ceramic inclusions with $\epsilon_i = 114$ permittivity were placed randomly in a homogenous background with $\epsilon_e = 3.7$ permittivity. Several different configurations were created by random simulations, and the electrostatic problem in the resulting geometry was solved using field-emission microscopy (FEM)-based electromagnetic software OPERA (Vector Fields). The domain was cubical and Dirichlet [perfect electric conductor (PEC)] and Neumann [perfect magnetic conductor (PMC)] boundary conditions were used on the boundaries. The static electric field was induced by applying the voltage $U_0 = 0$ on one side of the cube and $U_0 = 1$ V on the opposite side. The boundary conditions correspond to the placement of a sample of composite inside an ideal capacitor. The Laplace equation was solved in the whole domain, and the effective permittivity ϵ_x

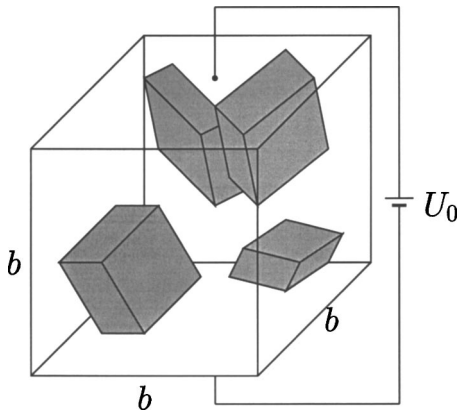

FIG. 6. Illutration of the computation domain. Inclusions with permittivity $\varepsilon_i=114$ (TiO_2) were placed randomly into an environment with permittivity $\varepsilon_e=3.7$ (epoxy), and a static electric field was applied. The boundary conditions were PEC and PMC, corresponding to an ideal capacitor.

of the composite was then determined by integrating over the side A, where $V=0$,

$$\epsilon_x = \frac{1}{bU}\int_A \mathbf{D}\cdot d\mathbf{A}, \tag{3}$$

where D is the electric flux and b the length of the side of the cube. Different volume fractions of ceramic powder were modeled by placing different numbers of particles into the environment. The volume fraction of inclusions was then solved by integrating over inclusions.

The average value of the unknowns was 30 000 in the simulations. More unknowns were used at the boundaries of the particles and the domain.

B. Averaging method

The modeled ceramic/polymer composite is isotropic on a large scale. However, numerical simulations made the samples anisotropic because of the restricted computation domain. The ideal capacitor shown in Fig. 6 corresponds to a periodic composite with periodicity b, where b is the side of the cube. Commonly, anisotropy is removed by choosing the computation domain to be very large compared to the size of the inclusions. In this study, instead, the effect of anisotropy was compensated for by using the method presented in Ref. 16. Every Monte Carlo sample is calculated with three separate runs with a field parallel to the x, y, or z axis, which results in three values of effective permittivity for the sample: ϵ_x, ϵ_y, and ϵ_z. With these estimates, the upper limit of the effective permittivity is

$$\epsilon_{\max} = \frac{1}{3}(\epsilon_x + \epsilon_y + \epsilon_z). \tag{4}$$

This corresponds to capacitors connected in parallel with respect to voltage. Respectively, capacitors connected in series correspond to the lower limit,

$$\epsilon_{\min} = 3\frac{\epsilon_x\epsilon_y\epsilon_z}{\epsilon_x\epsilon_y + \epsilon_y\epsilon_z + \epsilon_z\epsilon_x}. \tag{5}$$

The average effective permittivity of the sample is then calculated as an average,

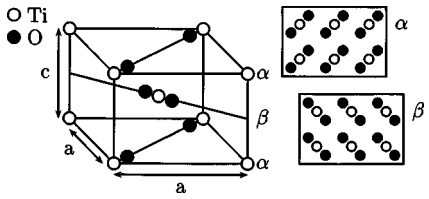

FIG. 7. The lattice structure of TiO_2 in a rutile phase is presented on the left. The planes α and β are identical with a rotation of $\pi/2$.

$$\epsilon_{\text{eff}} = (\epsilon_{\min} + \epsilon_{\max})/2. \tag{6}$$

This procedure compensates very effectively for anisotropy in the simulations, and consequently, larger-scale isotropy is better modeled. It was shown[16] that, for spherical inclusions, which are allowed to overlap each other, and for the boundaries of the domain, the size of the domain compared to the radii of the spheres could be quite small, and the effective permittivity was still captured with reasonable accuracy. The dimension of inclusions can be up to the order of $0.4b$.

C. Modeling fine structure

The structure used in numerical simulations should correspond to the fine structure of the real TiO_2/epoxy composite. In this study, the model took into account the fine structure as realistically as possible. The assumption was that the shape of elementary inclusions is the most important parameter. The other parameters, including the size distribution and clustering effects, play a minor role. However, clusterization is modeled by random positions of inclusions, which allows some overlap. This is, indeed, common in densely packed ceramic/polymer composites.

The average shape of inclusions is assumed to rise from the lattice structure of the rutile phase. The distance between titanium and oxygen atoms is about $0.07a$,[17] where a is the lattice constant (4.6 Å), as presented in Fig. 7. The height c compared to the length a in a unit cell is $c/a=0.57$. The distance between oxygen and titanium atoms is small compared to the other distances. The planes α and β are identical, with the exception of the separation $a/2$ and rotation of $\pi/2$. Because of this symmetry, particles are assumed to follow the shape presented in Fig. 8, which corresponds to the unit cell in the α or β plane. The distance between these planes is $c/(2a)=0.28$, and the lattice constant of the plane is a. The distance to the nearest titanium and oxygen atoms is the largest, and the dimensions are $w=a$, $l=a$, and $h=0.28a$. This prism is the basic shape used in numerical simulations.

The inclusions are placed randomly into a cubical environment. They can cross the boundaries and touch each

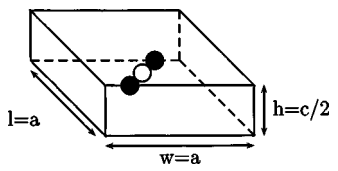

FIG. 8. The smallest cell, which contains a titanium atom and two oxygen atoms.

other, but they cannot penetrate into each other. In the simulations, this is done by defining seven equally spaced points on all edges of the prisms: $p_1, \ldots, p_7$. It is then ensured that these points are not inside any other prism. The point p_n is inside a convex particle defined by surfaces with normal vectors $\mathbf{n}_1, \ldots, \mathbf{n}_M$ if

$$\frac{\mathbf{r}_n \cdot \mathbf{n}_i}{\sqrt{\mathbf{r}_n \cdot \mathbf{n}_i}} > 0, \tag{7}$$

for all $i=1, \ldots, M$, where $\mathbf{r}_n$ is a vector pointing from p_n to the surface, where the normal vector is $\mathbf{n}_i$. If a new prism has an edge point inside any prism already placed in the composite, this new prism is rejected. It is also rejected if any prism has an edge point inside this new prism.

The basic shape presented in Fig. 8 is an average shape. Some deviation was allowed in order to be able to model large mixing ratios. Every side of the prism has a normally distributed random value with expectation values of w, l, and h, as in Fig. 8, and variances $\sigma=0.07w$, $0.07l$, and $0.07h$. The expectation values compared to the side of the cube were chosen according to[16] $w=l=0.4a$. The deviation mainly has an effect on the deviation of simulated effective permittivities, but not the estimated average values. On the other hand, a smaller deviation in the sample volumes makes the simulations slower, because for a large volume fraction of inclusions, smaller prisms are needed to fill the empty space between the existing inclusions.

D. Compensation of air content: Classical mixing rules

The effect of the air content in TiO_2/epoxy composites was eliminated analytically before comparison with the simulations. The classical mixing formulas were used. These formulas predict the macroscopic permittivity of mixtures with spherical inclusions and low volume fractions. The unified mixing formula[4] for the effective permittivity of a mixture is

$$\frac{\epsilon_{\text{eff}} - \epsilon_e}{\epsilon_{\text{eff}} + 2\epsilon_e + \nu(\epsilon_{\text{eff}} - \epsilon_e)} = p\frac{\epsilon_i - \epsilon_e}{\epsilon_i + 2\epsilon_e + \nu(\epsilon_{\text{eff}} - \epsilon_e)}, \tag{8}$$

where ϵ_i is the permittivity of inclusions, ϵ_e the permittivity of the environment, and p the volume fraction of inclusions. The parameter ν has different values for the classical mixing equations: $\nu=0$ for Maxwell Garnett, $\nu=2$ Bruggeman, and $\nu=3$ for the coherent potential formula. In this study, the air bubbles were well separated and spherical, and their volume fraction was small. Accordingly, the Maxwell–Garnett mixing formula could be used. Thus, in Eq. (8) $\nu=0$, ϵ_i is the permittivity of air, p is the volume fraction of air, ϵ_{eff} is the measured permittivity, and ϵ_e is the permittivity of a pure TiO_2/epoxy composite, which is solved. The volume fraction of air content was solved by making use of information of the total volume of a sample V_{tot}, the density of epoxy ρ_e, the density of TiO_2, ρ_t, the mass of epoxy m_e, and the mass of TiO_2, m_t.

E. Difference between measured and numerically modeled permittivities

To be able to estimate how well the simulations agree with the measured effective permittivity of the TiO_2/epoxy composite, an empirical logaritmic equation was fitted to the simulated effective permittivities,

$$\epsilon_{\text{eff}} = \epsilon_e 10^{x_1 p^{2+x_2 p}}, \tag{9}$$

where ϵ_e is the permittivity of epoxy, p is the volume fraction of TiO_2 inclusions, and x_1 and x_2 are the parameters to be fitted. The fitting was done by using the least-squares method for the set of modeled effective permittivities after averaging over ϵ_x, ϵ_y, and ϵ_z. The average of the measured effective permittivities ϵ_{meas} can then be compared to the fitted permittivity (9) using relative difference,

$$\Delta = \frac{\epsilon_{\text{meas}} - \epsilon_{\text{fit}}}{\epsilon_{\text{fit}}}. \tag{10}$$

F. Effective-medium models for suspension of ellipsoids

Mixing principles according to Eq. (8) assume the shape of the inclusions to be spherical. This describes poorly the shape of real TiO_2 inclusions. A better model for these is certainly ellipsoidal. Motivated by the lattice properties of TiO_2, we take the ellipsoidal inclusions to be oblate spheroids (ellipsoids of revolution) with the same axis ratio as the prisms had in the simulations: $a_x=a_y$ and $a_z/a_x=0.28$ and use an analytical mixing formula.

The depolarization factors for oblate spheroids read

$$N_z = \frac{1+e^2}{e^3}(e - \arctan e), \quad N_x = N_y = \frac{1}{2}(1 - N_z), \tag{11}$$

where the eccentricity is $e=\sqrt{a_x^2/a_z^2 - 1}$. Maxwell Garnett mixing rule (Ref. 4, Sec. 4.2.4) for randomly oriented ellisoids is

$$\epsilon_{\text{eff}} = \epsilon_e + \epsilon_e \frac{p \sum_{j=x,y,z} \frac{\epsilon_i - \epsilon_e}{\epsilon_e + N_j(\epsilon_i - \epsilon_e)}}{3 - p \sum_{j=x,y,z} \frac{N_j(\epsilon_i - \epsilon_e)}{\epsilon_e + N_j(\epsilon_i - \epsilon_e)}}, \tag{12}$$

which is the same equation as the mixing rule by Fricke [Ref. 18, Eq. (31)] for a suspension of randomly oriented ellipsoids.

A modification of this mixing rule (12) can be derived if it is applied iteratively. The environment is filled stepwise with smaller and smaller ellipsoids. The background is homogenized along with each step. Then the homogenized background becomes the environment for the new set of ellipsoids. The iterative solution for the effective permittivity ϵ_{eff} after K iteration steps is $\epsilon_{\text{eff},K}$. The volume fraction of inclusions is p and instantaneous volume fraction during iteration p_k, where index $k=0 \cdots K$.

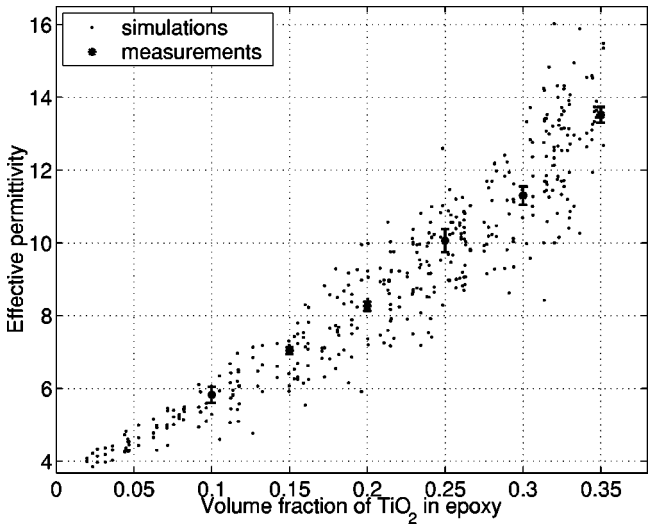

FIG. 9. Modeled (dots) and measured (asterisks) effective permittivities for TiO_2/epoxy composite. The deviations of the measured permittivities were calculated using Eq. (2). In the simulations, the field solution for each Monte Carlo sample was calculated three times, corresponding to the three orthogonal field excitations. Accordingly, for every volume fraction, permittivities of ε_x, ε_y, and ε_z are presented.

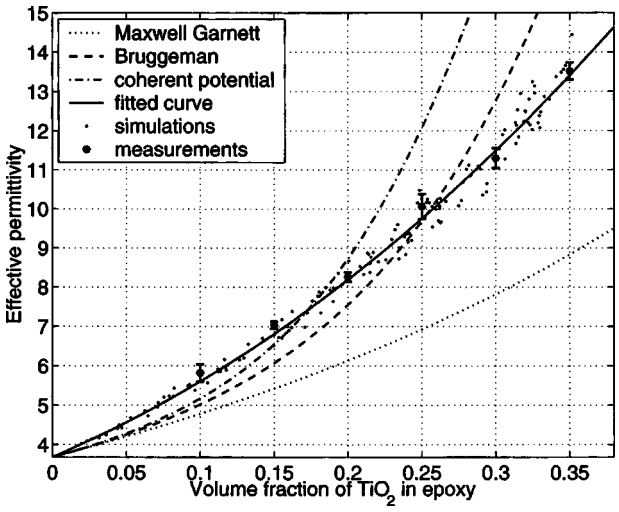

FIG. 10. Modeled (dots) and measured (asterisks) effective permittivities of TiO_2/epoxy composite, as in Fig. 9, but now the simulated permittivities are shown averaged over ε_x, ε_y, and ε_z according to Eq. (6) for every Monte Carlo sample. Equation (9) was fitted to the simulations and is marked with a solid line.

$$p_k = \frac{p}{K(1-p)+kp}. \tag{13}$$

The total number of iterations should be chosen so that the effective permittivity does not change noticeably when the number of iteration steps is increased. The iteration algorithm to calculate the effective permittivity of the mixture is

$$\epsilon_{\mathrm{eff},k+1} = \epsilon_{\mathrm{eff},k} + \epsilon_{\mathrm{eff},k} \frac{p_k \sum_{j=x,y,z} \frac{\epsilon_i - \epsilon_{\mathrm{eff},k}}{\epsilon_{\mathrm{eff},k} + N_j(\epsilon_i - \epsilon_{\mathrm{eff},k})}}{3 - p_k \sum_{j=x,y,z} \frac{N_j(\epsilon_i - \epsilon_{\mathrm{eff},k})}{\epsilon_{\mathrm{eff},k} + N_j(\epsilon_i - \epsilon_{\mathrm{eff},k})}}, \tag{14}$$

and the starting value is $\epsilon_{n,0} = \epsilon_e$.

IV. RESULTS AND DISCUSSION

In Fig. 9, the modeled and measured effective permittivities of a TiO_2/epoxy composite are presented as functions of the volume fractions of TiO_2 powder. For 10, 15, 20, 25, 30, and 35 vol % volume fraction of TiO_2, $4\cdots6$ samples were measured and the effect of air content was removed from the measurement results. The measured effective permittivities are marked with asterisks and the deviations with lines [Eq. (2)]. The modeled effective permittivity is presented without averaging over ϵ_x, ϵ_y, and ϵ_z, and for every volume fraction of TiO_2 powder, therefore, three points can be seen. The deviation is very large because every Monte Carlo sample is anisotropic. When the computation domain decreases compared with the inclusions, anisotropy increases. However, the anisotropy is effectively compensated for by averaging over ϵ_x, ϵ_y, and ϵ_z.

In Fig. 10, the simulated effective permittivity is presented after the averaging. Now the deviation of the simulations is reasonably small, and the simulations and the measurements are in a very good agreement over all volume fractions of inclusions. As a comparison, the predictions of the classical mixing formulas (8) are also presented. They underestimate the effective permittivity in the region of low volume fractions. This is to be expected because the polarizability of TiO_2 particles is higher than the polarizability of a sphere, which is the assumed element shape for the mixing models. On the other hand, mixing formulas are based on the assumption of low volume fractions and therefore they generally fail for dense mixtures. Overall, it can be concluded that none of the formulas predicts well the permittivity of the TiO_2/epoxy composite.

The logarithmic Eq. (9) was fitted to the simulated effective permittivities using the least-squares method. The fitted parameters are $x_1 = -0.8898$ and $x_2 = 1.9156$. The measured permittivities are compared to this simulation curve using the relative difference (10). For 10, 15, 20, 25, 30, and 35 vol % of TiO_2 particles, the relative differences are 0.0387, 0.0334, 0.0082, 0.0318, −0.0168, and 0.0084.

Figure 11 shows the performance of the advanced mixing models in predicting the effective permittivity. Both the basic [Maxwell Garnett (MG) for ellipsoids[12]] and the incremental (MG for ellipsoids iteration[14]) estimates are shown. Instead of prisms, now the composite is modeled as a suspension of oblate spheroids. The curve fitted to the numerical simulations is presented with a solid line, which lies in between the analytical solutions for the most part of the volume fraction range. The result shows that the incremental effective-medium model gives a reasonable estimate to the effective permittivity of the composite.

As a reminder of the modeled microstructure in the numerical simulations, the expectation shape was a prism with sides (1:1:0.28). The longer side of the prism had an expectation value of $0.4b$, where b was the side of the cubical computation domain. Accordingly, the computation domain is relatively small, which is a major advantage when computing in three dimensions. For example, halving of the size

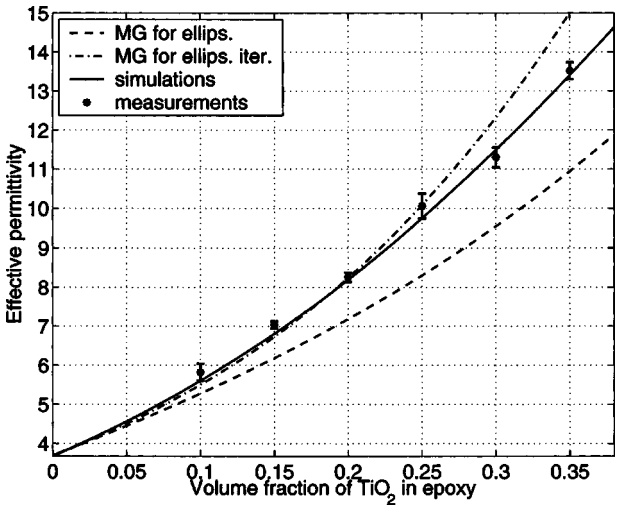

FIG. 11. Maxwell Garnett effective-medium model applied directly (dashed) and iteratively (dash-dotted line) for the mixture with randomly oriented spheroids.

of the inclusions would require eight times more unknowns with the same numerical accuracy. In the finite-element method, this means more than eightfold multiplication of computation time.

The agreement between the measured and simulated effective permittivities is excellent. The relative difference between the average measured permittivity and the curve fitted to the simulations is less than 4% with all measured volume fractions of inclusions, which is of the same order as the uncertainty in the measurements. It is important to note that the modeling results were calculated directly from the geometry of the elementary inclusions and the permittivities of TiO_2. The axis ratio in the advanced effective-medium models was also calculated from the lattice structure. No adjustable parameters were needed in numerical or analytical models.

Finally, the numerical method is not restricted to the FEM algorithm used here, but it could also be used with other numerical methods, such as finite-difference time domain (FDTD). In the numerical evaluation of permittivities, it is essential that every simulated sample is calculated with three separate runs using three orthogonal field directions. Note that even if in the present study the advanced mixing models gave a reasonable prediction for the effective permittivity, this may not be the case if the approximation of the inclusion prisms by ellipsoids is no longer realistic. In that case one has to revert to full numerical simulations with which any geometries and inclusion shapes can be considered.

V. CONCLUSIONS

This paper presents the results of a study with two objectives: to determine both the measured and the simulated effective permittivities of composites where titanium oxide inclusions occupy a given volume in a neutral epoxy matrix. The samples were prepared with care, including isotropic distribution of the inclusion phase. The microstructure of the resulting samples was analyzed.

On the modeling side, the input data consisted of the permittivities of the two phases of the composite and the shape of the ceramic inclusions. Particular attention was paid to the crystallographic lattice of the TiO_2 phase in order to ensure the most realistic parameters in the model for the mixture. The prism-shaped elements were dispersed randomly—both in orientation and in position—in the Monte Carlo simulations to create virtual samples that would represent the composite.

With a finite-element code, the electrostatic problem was solved, leading to a numerical estimate of the effective permittivity of each sample. The averaging method was exploited to reduce considerably the cost of computations. The agreement of the modeling results with the experimental data testifies strongly for the applicability of the numerical model.

This study shows also that the ceramic-polymer composites can be modeled analytically without any parametric fitting if only the microstructure of the material is carefully accounted for. In addition to the fact that the numerical simulations were in an excellent agreement with the measurements. It was shown that analytical solution with the incremental Maxwell Garnett mixing formula for a suspension of ellipsoids also gives a reasonable agreement.

ACKNOWLEDGMENTS

This work was part of the Academy of Finland Project Nos. 206123 and 121598. The numerical calculations were performed using computers of the Finnish IT Center for Science (CSC).

[1]P. Chalal, R. R. Tummala, M. G. Allen, and M. Swaminathan, IEEE Trans. Compon., Packag. Manuf. Technol., Part B **21**, 184 (1998).
[2]C. Dias, R. Igreja, R. Marat-Mendes, P. Incio, J. Marat-Mendes, and D. K. Das-Gupta, IEEE Trans. Dielectr. Electr. Insul. **11**, 35 (2004).
[3]G. Milton, *The Theory of Composites* (Cambridge University Press, Cambridge, 2002).
[4]A. Sihvola, *Electromagnetic Mixing Formulas and Applications*, IEE Electromagnetic Waves Series 47 (The Institution of Electrical Engineers, London, 1999).
[5]R. Diaz, W. Merrill, and N. Alexopoulos, J. Appl. Phys. **84**, 6815 (1998).
[6]E. Tuncer, Y. V. Serdyuk, and S. M. Gubanski, IEEE Trans. Dielectr. Electr. Insul. **9**, 809 (2002).
[7]Y. Wu, X. Zhao, F. Li, and Z. Fan, J. Electroceram. **11**, 227 (2003).
[8]L. Pardo, J. Mendiola, and C. Alemany, J. Appl. Phys. **64**, 5092 (1988).
[9]K. K. Kärkkäinen, A. H. Sihvola, and K. I. Nikoskinen, IEEE Trans. Geosci. Remote Sens.38, 1303 (2000).
[10]I. Krakovsky and V. Myroshnychenko, J. Appl. Phys. **92**, 6743 (2002).
[11]B. Sareni, L. Krähenbhl, and A. Beroual, J. Appl. Phys. **81**, 2375 (1997).
[12]C. Dias and D. Das-Gupta, IEEE Trans. Dielectr. Electr. Insul. **3**, 706 (1996).
[13]S. Orlowska, A. Beroual, and J. Fleszynski, J. Phys. D **35**, 2656 (2002).
[14]R. Parker, Phys. Rev. **124**, 1719 (1961).
[15]N. Klein, C. Zuccaro, U. Dähne, H. Schulz, N. Tellmann, R. Kutzner, A. G. Zaitsev, and R. Wödenwber, J. Appl. Phys. **78**, 6683 (1995).
[16]L. Jylhä and A. Sihvola, IEEE Trans. Geosci. Remote Sens. 43, 59 (2005).
[17]S. Ogata, H. Iyetomi, K. Tsuruta, F. Shimojo, R. K. Kalia, A. Nakano, and P. Vashishta, J. Appl. Phys. **86**, 3036 (1999).
[18]H. Fricke, J. Phys. Chem. **57**, 934 (1953).